# Manipulating and Quantifying the Compositional Heterogeneity in Sol−Gel Processed $K(Ta_{1-x}Nb_x)O_3$

Jie Xu, Angus P. Wilkinson,* and Sidhartha Pattanaik†

*School of Chemistry & Biochemistry, Georgia Institute of Technology, Atlanta, Georgia 30332-0400*

*Received June 9, 2000. Revised Manuscript Received January 23, 2001*

A series of $K(Ta_xNb_{1-x})O_3$ (KTN) samples were prepared by two different sol−gel processes and by the reaction of mixed oxides. The local and long-range structures of the sol−gel-processed materials were examined as a function of heat treatment using a combination of powder diffraction and EXAFS studies. The compositional homogeneity of the perovskite solid solution products was also examined by EXAFS. The local structures around both the niobium and tantalum in the sol−gel-processed samples change on heating prior to crystallization. EXAFS provided evidence for the existence of Ta−O−Nb links in the dry KTN gels. The data for the perovskite KTN samples prepared using a conventional alkoxide sol−gel route are consistent with a random distribution of tantalum and niobium in the solid solution. However, the materials prepared by the direct reaction of mixed oxides were highly inhomogeneous, even after several regrinding and heating cycles. An alternative sol−gel method that employed prehydrolyzed precursors was successfully used to deliberately introduce compositional inhomogeneities into KTN specimens.

## Introduction

The compositional homogeneity of a material can have a profound effect on its properties. In the case of ferroelectrics, compositional fluctuations over a short length scale have been implicated in the relaxor behavior of materials such as $Pb(Mg_{1/3}Nb_{2/3})O_3$ (PMN),[1−6] and variations in the composition within bulk samples influence the temperature dependence of the dielectric constant for solid solutions such as $K(Ta_{1-x}Nb_x)O_3$ (KTN) and $Pb(Zr_{1-x}Ti_x)O_3$ (PZT). This arises because the ferroelectric-to-paraelectric phase transition temperature is composition-dependent.[7]

Typically, solution-processing routes, such as alkoxide-based sol−gel methods, are employed with the goal of obtaining materials that display good compositional homogeneity. However, the use of sol−gel chemistry does not guarantee the compositional homogeneity of the end product. The homogeneity of a sol or gel might depend on kinetic factors. In multicomponent precursor solutions, different rates of hydrolysis or metal−oxygen−metal link formation could lead to compositional heterogeneity. There have been reports from other workers that sol−gel methods do not always deliver compositionally homogeneous materials,[8−10] and our previous studies of $Pb(Zr_xTi_{1-x})O_3$ (PZT)[11] and $Ca(Zr_xTi_{1-x})O_3$ (CZT)[12] have shown that both the xerogels and crystalline samples prepared by conventional sol−gel methods can display some heterogeneity.

To better understand how sol−gel chemistry can be used to control the compositional homogeneity of solid solutions, we extended our studies to $K(Ta_xNb_{1-x})O_3$ (KTN). This system was selected because of its intrinsically interesting physical properties and the expectation that the very similar charge-to-size ratios of $Ta^{5+}$ and $Nb^{5+}$ would lead to identical hydrolysis and metal−oxygen−metal link formation kinetics for the two metals. This was not the case in the zirconium titanate systems that we have previously studied; titanium alkoxides undergo hydrolysis much more rapidly than the corresponding zirconium compounds.

Sol−gel methods have previously been used for the synthesis of bulk and thin-film KTN. For example, Yogo et al. reported the synthesis of highly oriented perovskite $K(Ta_{0.65}Nb_{0.35})O_3$ thin films on Pt(100)/MgO(100) substrates at 700 °C using an ethoxide solution,[13,14] and Lu et al. synthesized KTN powders and thin films on different substrates using ethoxide precursors. Typically, perovskite KTN crystallizes at ∼750 °C when prepared in this way.[15−17]

* Author to whom correspondence should be addressed.
† Present address: The Consortium for Fuel Liquefaction Science, University of Kentucky, Room 111, 533 South Limestone Street, Lexington, KY 40506-0043.

(1) Isupov, V. A. *Sov. Phys.—Technol. Phys.* **1956**, *1*, 1846−1849.
(2) Rolov, B. N. *Sov. Phys. Solid State* **1965**, *6*, 1676−1678.
(3) Smolensky, G. A. *J. Phys. Soc. Jpn.* **1970**, *S28*, 26−37.
(4) Setter, N.; Cross, L. E. *J. Appl. Phys.* **1980**, *51*, 4356−4360.
(5) Kirillov, V. V.; Isupov, V. A. *Ferroelectrics* **1973**, *5*, 3−9.
(6) Cross, L. E. *Ferroelectrics* **1987**, *76*, 241−267.
(7) Jona, F.; Shirane, G. *Ferroelectric Crystals*; Dover Publications: Mineola, NY, 1993.
(8) Sengupta, S. S.; Ma, L.; Adler, D. L.; Payne, D. A. *J. Mater. Res.* **1995**, *10*, 1345−1348.
(9) Lakeman, C. D. E.; Xu, Z.; Payne, D. A. *J. Mater. Res.* **1995**, *10*, 2042−2051.
(10) Tuttle, B. A.; Headley, T. J.; Bunker, B. C.; Schwartz, R. W.; Zender, T. J.; Hernandez, C. L.; Goodnow, D. C.; Tissot, R. J.; Michael, J. *J. Mater. Res.* **1992**, *7*, 1876−1882.
(11) Wilkinson, A. P.; Xu, J.; Pattanaik, S.; Billinge, S. J. L. *Chem. Mater.* **1998**, *10*, 3611−3619.
(12) Xu, J.; Pattanaik, S.; Wilkinson, A. P. *Chem. Mater.* **2000**, *12*, 3321−3330.
(13) Yogo, T.; Kikuta, K.; Ito, Y.; Hirano, S.-I. *J. Am. Ceram. Soc.* **1995**, *78*, 2175−2179.
(14) Hirano, S.-I.; Yogo, T.; Kikuta, K.-I.; Morishita, T.; Ito, Y. *J. Am. Ceram. Soc.* **1992**, *75*, 1701−1704.

10.1021/cm0004735 CCC: $20.00 
Published on Web 03/24/2001

In the current paper, we compare the effects of two different sol−gel procedures on the B-site cation distribution in 50:50 KTN and explore the use of EXAFS as both a qualitative and a quantitative tool for the examination of a solid solution's inhomogeneity. Preliminary results from this work have already been published as conference proceedings.[18] The two sol−gel methods examined were a homogeneous process, in which all of the starting materials were mixed together to produce a solution prior to hydrolysis, and an inhomogeneous method, in which $KTaO_3$ and $KNbO_3$ precursor solutions were made and partially hydrolyzed prior to mixing. The latter route was examined to determine whether compositional inhomogeneity could be deliberately introduced and maintained in the final products after heat treatment. Additionally, several KTN compositions prepared by conventional sol−gel methods and two KTN 50:50 samples prepared by the direct reaction of metal oxides were examined for comparison purposes.

Quantifying the "compositional inhomogeneity" in a solid solution is intrinsically difficult; it is impossible to specify the exact distribution of metal ions in a material such as $K(Ta_{1-x}Nb_x)O_3$. However, some progress can be made by determining the probability that an ion in the solid solution at some distance $R$ from a specified atom type will be either Nb or Ta. In principle, EXAFS can be used to experimentally determine this probability for small values of $R$. At large distances, the Fourier transform magnitudes become increasingly complex and very noisy. The current work is confined to a consideration of nearest-neighbor transition metal ions.

EXAFS has not previously been used to examine the sol−gel processing of KTN. However, it has been employed to study phase transitions in this system. For example, Stern et al.[19,20] examined the effects of temperature and hydrostatic pressure on the off-center niobium displacements in $KTa_{0.91}Nb_{0.09}O_3$. This work showed that the niobium is always displaced along the [111] direction, even at temperatures where the structure is macroscopically cubic.

## Experimental Section

**Syntheses.** $Nb(OEt)_5$ and $Ta(OEt)_5$ were prepared using literature methods.[21,22] They were dissolved in 2-methoxyethanol (Aldrich) to make 0.839 M niobium and 0.515 M tantalum alkoxide stock solutions.

*Conventional Mixed Alkoxide Syntheses.* Samples with the compositions $K(Nb_{0.96}Ta_{0.04})O_3$, $K(Nb_{0.67}Ta_{0.33})O_3$, $K(Nb_{0.50}Ta_{0.50})O_3$, $K(Nb_{0.33}Ta_{0.67})O_3$, and $K(Nb_{0.04}Ta_{0.96})O_3$ were prepared. As a similar procedure was used in each case, details are only given for the 50:50 sample.

Potassium acetate (2.84 g) was dissolved in ∼100 mL of 2-methoxyethanol and refluxed for 1 h. Approximately 54 mL of the solvent mixture was then removed by distillation. Stoichiometric amounts of the niobium and tantalum alkoxide stock solutions were then added. 2-Methoxyethanol (10 mL) was used to wash any residue into the flask. The mixture was then briefly refluxed, and ∼57 mL of solvent was distilled out to concentrate the solution. Acetylacetone (1.49 mL) was added to the mixture prior to hydrolysis (acac:metal alkoxide = 0.5:1). For the hydrolysis, 2.1 mL of $H_2O$ diluted to 10 mL using 2-methoxyethanol was used ($H_2O$:metal alkoxide = 4:1). The water-containing solution was added dropwise. A gel was obtained after 30 h. It was dried under vacuum at 110 °C for ∼12 h. Portions of dried gel were heated at 5 °C/min to 400, 500, 600, 700, and 1000 °C and held at the final temperature for 5 h.

*KT and KN Precursor Solutions.* Potassium acetate (3.54 g) was dissolved in ∼100 mL of 2-methoxyethanol and refluxed for 1 h. Approximately 53 mL of solvent mixture was removed by distillation. Then, 70.09 mL of the tantalum alkoxide stock solution was added. 2-Methoxyethanol (10 mL) was used to wash any residue into the flask. The mixture was refluxed, and 46 mL of solvent was removed by distillation. The concentration of the KT precursor solution was determined gravimetrically to be 0.383 M. A 0.534 M KN precursor solution was prepared in a similar fashion. Portions of the precursor solutions were used to prepare $KTaO_3$ and $KNbO_3$; some of the remaining material was prehydrolyzed and used to prepare KTN 50:50.

*Preparation of $K(Nb_{0.50}Ta_{0.50})O_3$ Using Prehydrolyzed Precursors.* Into separate flasks were measured 37.45 mL of the KN and 52.22 mL of the KT precursor solutions. Acetylacetone (0.1 mL) was added to each flask to lower the hydrolysis rate. A solution of 1.45 mL of water (water:alkoxide 4:1) diluted to 18 mL with 2-methoxyethanol was used to hydrolyze the KN precursor. This gave a final niobium concentration of 0.33 M. Next, 1.45 mL of water diluted to 5 mL with 2-methoxyethanol was added to hydrolyze the KT precursor, giving a final concentration of 0.33 M. The KN solution partially gelled after 5 min (becoming very viscous), whereas the KT solution was less viscous. At this time, the precursors were mixed and stirred for 5 min. The mixture was dried under vacuum overnight at 110 °C. Portions of dry gel were heated at 5 °C/min to 400, 500, 600, 700, and 1000 °C for 5 h. Samples were also prepared by heating portions of the gel at 1000 °C for 1, 2, 4, and 8 h.

*Direct Reaction of Mixed Oxides and Carbonates.* Two different $K(Ta_{0.5}Nb_{0.5})O_3$ samples were prepared from mixed oxides. One (sample C3) was prepared by mixing stoichiometric amounts of $K_2CO_3$, $Nb_2O_5$, and $Ta_2O_5$, grinding the mixture by hand, and heating it to 1000 °C for 20 h. The second sample (C4) was prepared by mixing and grinding the reagents for 1 h, pressing the mixture into a pellet, and heating the pellet to 1000 °C for 10 h; grinding the material and heating it to 1100 °C for an additional 10 h; and finally grinding and heating the sample to 1000 °C for another 10 h. $KTaO_3$ and $KNbO_3$ samples were also prepared by the direct reaction of oxides and carbonates.

(15) Lu, C. J.; Kuang, A. X. *J. Mater. Sci.* **1997**, *32*, 4412−4427.
(16) Liu, D. D.; Ho, J. G.; Pastor, R. C.; Stafsudd, O. M. *Mater. Res. Bull.* **1992**, *27*, 723−729.
(17) Kuang, A. X.; Lu, C. J.; Huang, G. Y.; Wang, S. M. *J. Cryst. Growth* **1995**, *149*, 80−86.
(18) Wilkinson, A. P.; Xu, J.; Pattanaik, S. *Mater. Res. Soc. Symp. Proc.* **1998**, *524*, 333−337.
(19) Hanske-Petitpierre, O.; Yacoby, Y.; Mustre de Leon, J.; Stern, E. A.; Rehr, J. J. *Phys. Rev. B* **1991**, *44*, 6700−6707.
(20) Wang, F.; Ravel, B.; Yacoby, E. A.; Stern, E. A.; Ingalls, R. *J. Phys. IV Fr.* **1997**, *7*, C2 1225−1226.
(21) Bradley, D. C.; Wardlaw, W.; Whitley, A. *J. Chem. Soc.* **1955**, 726−728.
(22) Bradley, D. C.; Chakravarti, B. N.; Wardlaw, W. *J. Chem. Soc.* **1956**, 2381−2384.

**Table 1. Samples Studied by EXAFS and $\Delta k$ ($Å^{-1}$) Available for Analysis**

| sample ID | composition | synthesis procedure[a] | $\Delta k$[b] Nb K-edge | $\Delta k$[b] Ta $L_{III}$-edge |
|---|---|---|---|---|
| C1 | $KTaO_3$ | mixed oxide, 1000 °C, 24 h | N/A | 1−17.74 |
| C2 | $KNbO_3$ | mixed oxide, 900 °C, 5 h | 1−21.66 | N/A |
| C3 | $K(Ta_{0.5}Nb_{0.5})O_3$ | mixed oxide, 1000 °C, 20 h | 1−21.08 | 1−17.73 |
| C4 | $K(Ta_{0.5}Nb_{0.5})O_3$ | mixed oxide, 1100 °C, 10 h | 1−19.44 | 1−17.61 |
| H1 | $K(Ta_{0.5}Nb_{0.5})O_3$ | homo SG dry gel | 1−19.25 | 1−17.46 |
| H2 | $K(Ta_{0.5}Nb_{0.5})O_3$ | homo SG, 500 °C, 5 h | 1−18.64 | 1−17.46 |
| H3 | $K(Ta_{0.5}Nb_{0.5})O_3$ | homo SG, 700 °C, 5 h | 1−19.64 | 1−17.71 |
| H4 | $K(Ta_{0.5}Nb_{0.5})O_3$ | homo SG, 1000 °C, 5 h | 1−19.76 | 1−17.67 |
| H5 | $K(Ta_{0.96}Nb_{0.04})O_3$ | homo SG, 1000 °C, 5 h | 1−19.60 | N/A |
| H6 | $K(Ta_{0.67}Nb_{0.33})O_3$ | homo SG, 1000 °C, 5 h | 1−19.32 | 1−17.62 |
| H7 | $K(Ta_{0.33}Nb_{0.67})O_3$ | homo SG, 1000 °C, 5 h | 1−19.26 | 1−17.40 |
| H8 | $K(Ta_{0.04}Nb_{0.96})O_3$ | homo SG, 1000 °C, 5 h | N/A | 1−17.47 |
| IH1 | $K(Ta_{0.5}Nb_{0.5})O_3$ | inhomo SG dry gel | 1−17.39 | 1−17.47 |
| IH2 | $K(Ta_{0.5}Nb_{0.5})O_3$ | inhomo SG, 500 °C, 5 h | 1−16.83 | 1−17.15 |
| IH3 | $K(Ta_{0.5}Nb_{0.5})O_3$ | inhomo SG, 700 °C, 5 h | 1−21.33 | 1−17.50 |
| IH4 | $K(Ta_{0.5}Nb_{0.5})O_3$ | inhomo SG, 1000 °C, 5 h | 1−21.56 | 1−17.73 |
| IH5 | $K(Ta_{0.5}Nb_{0.5})O_3$ | inhomo SG, 1000 °C, 1 h | 1−19.54 | 1−17.37 |
| IH6 | $K(Ta_{0.5}Nb_{0.5})O_3$ | inhomo SG, 1000 °C, 2 h | 1−19.39 | 1−17.71 |
| IH7 | $K(Ta_{0.5}Nb_{0.5})O_3$ | inhomo SG, 1000 °C, 4 h | 1−19.36 | 1−17.66 |
| IH8 | $K(Ta_{0.5}Nb_{0.5})O_3$ | inhomo SG, 1000 °C, 8 h | 1−18.88 | 1−17.68 |
| S1 | $KTaO_3$ | SG dry gel | N/A | 1−17.49 |
| S2 | $KNbO_3$ | SG dry gel | 1−19.13 | N/A |

[a] SG = sol−gel; homo = homogeneous; inhomo = inhomogeneous. [b] N/A = not applicable.

**Characterization.** *Powder X-ray Diffraction.* All of the data were collected using a Scintag X1 instrument equipped with a Peltier cooled solid-state detector and employing Cu Kα radiation.

*Elemental Analyses.* The KTN, KN, and KT samples were dissolved in HF and analyzed using a Perkin-Ellmer Optima 3000 ICP-AES instrument.

*EXAFS Measurements.* Nb K-edge and Ta $L_{III}$-edge spectra were recorded in transmission mode using beamline X11A at the National Synchrotron Light Source, Brookhaven National Laboratory. A Si(111) double-crystal monochromator and a beam size of 10 × 1 $mm^2$ were used for all of the measurements. The spectra were obtained using a three-ion-chamber arrangement, with the sample between the first two detectors and a reference foil between the second and third detectors. All of the samples were cooled to approximately −50 °C. Harmonic rejections of 20% $I_0$ and 40% $I_0$ were used for the Nb K-edge and Ta $L_{III}$-edge spectra, respectively. Three scans were acquired for each sample and averaged prior to analysis. A summary of the data collected and the naming scheme for the samples is presented in Table 1.

*EXAFS Data Analysis.* All of the data were processed using the package EXAFSPAK.[23] Phase shifts and scattering amplitude functions were obtained using the program FEFF7.[24] Rhombohedral $KNbO_3$ was used as the model structure for the analyses of the Nb K-edge data from all of the crystalline KTN samples, regardless of sample composition. It has previously been shown that the local structure around niobium in KTN is, to some extent, independent of temperature and solid-solution composition.[25,26] A local environment similar to that in rhombohedral $KNbO_3$ seems to be appropriate under most conditions. Cubic $KTaO_3$ was used as the model for the local structure around tantalum in all of the crystalline KTN specimens. $KTaO_3$ is macroscopically cubic at all temperatures, and previous EXAFS studies have shown that the local structure of $KTaO_3$ is cubic at all temperatures.[27] For the KTN compositions examined by EXAFS, there is very little distortion of the tantalum coordination environment.[19,20]

Mutliple scattering (MS) was taken into account during the quantitative analysis of the EXAFS data beyond the first shell. MS can be very important when atoms are arranged in a collinear fashion such as in the ideal perovskite structure.[28,29] Multiple scattering contributes more than 60% of the total backscattering from the first three shells in cubic $KTaO_3$. In our modeling, we included double scattering of the type $M_0-M_3-O_1$ (the subscript refers to the shell number and M = Nb or Ta) and triple scattering of the type $M_0-O_1-M_3-O_1$.

The phase and amplitude functions for the analysis of the Ta $L_{III}$-edge EXAFS data on the perovskite samples were obtained using a simple model generated by replacing some of the tantalum in the cubic $KTaO_3$ crystal structure with niobium. Appropriate values of $\Delta E_o$ for the paths Ta−O, Ta−K, and Ta−Ta were obtained by fitting the data for cubic $KTaO_3$. These values were used for all of the paths of equivalent length in the KTN data analyses. The distances for the $Ta_0-Ta_3$, $Ta_0-Nb_3$, $Ta_0-Ta_3-O_1$, $Ta_0-Nb_3-O_1$, $Ta_0-O_1-Ta_3-O_1$, and $Ta_0-O_1-Nb_3-O_1$ scattering paths were constrained to be the same as one another, and the Debye−Waller factors for the scattering paths Ta−M ($Ta_0-Ta_3$ and $Ta_0-Nb_3$), Ta−M−O ($Ta_0-Ta_3-O_1$ and $Ta_0-Nb_3-O_1$), and Ta−O−M−O ($Ta_0-O_1-Ta_3-O_1$ and

(23) George, G. N.; Pickering, I. J. *EXAFSPAK: A Suite of Programs for Analysis of X-ray Absorption Spectra*; SSRL: Stanford, CA, 1995.
(24) Zabinsky, S. I.; Rehr, J. J.; Ankubinov, A.; Albers, R. C.; Eller, M. J. *Phys. Rev. B* **1995**, *52*, 2995.
(25) de Mathan, N.; Prouzet, E.; Husson, E.; Depert, H. *J. Phys. Condens. Matter* **1993**, *5*, 1261−1270.
(26) Frenkel, A. I.; Wang, F. M.; Kelly, S.; Ingalls, R.; Haskel, D.; Stern, E. A.; Yacoby, Y. *Phys. Rev. B* **1997**, *56*, 10869−10877.
(27) Nishihata, Y.; Kamishima, O.; Ojima, K.; Sawada, A.; Maeda, H.; Terauchi, H. *J. Phys. Condens. Matter* **1994**, *6*, 9317−9328.
(28) Mustre, J.; Yacoby, Y.; Stern, E. A.; Rehr, J. J. *Phys. Rev. B.* **1990**, *42*, 10843−10851.
(29) Newville, M.; Ravel, B.; Haskel, D.; Rehr, J. J.; Stern, E. A.; Yacoby, Y. *Phys. B.* **1995**, *208 & 209*, 154−156.

$Ta_0-O_1-Nb_3-O_1$) were also constrained to be the same. Furthermore, the numbers of Ta−Ta and Ta−Nb, Ta−Ta−O and Ta−Nb−O, and $Ta_0-O_1-Ta_3-O_1$ and $Ta_0-O_1-Nb_3-O_1$ paths were constrained to be 6, 12, and 6, respectively. Using these constraints, the total number of variables was much less than the maximum number that could, in principle, be determined from the available data.[28,30] Such a simple model is clearly an approximation to the real situation, as it does not allow for any displacements of the tantalum or niobium atoms from the ideal perovskite positions. However, its simplicity makes a quantitative analysis feasible. A quantitative analysis of the Nb K-edge data including metal backscattering was not attempted.

## Results and Discussion

**Elemental Analyses.** The final crystalline products from the sol−gel syntheses all had the desired stoichiometries.

**Powder X-ray Diffraction Data.** Phase-pure perovskite was obtained after a 600 °C treatment of the 50:50 dry gel prepared by the conventional sol−gel route, whereas trace amounts of pyrochlore were found in the corresponding sample prepared using prehydrolyzed precursors. Pure perovskite was not obtained until the gel prepared by the latter route had been heated to 1000 °C for 5 h. The slightly different crystallization pathways suggest that the local structures of the two gels were different. The formation of an intermediate pyrochlore phase is commonly observed during the preparation of KTN.[14−17,31−33] Its formation and transformation to perovskite depends on the composition,[14] heat treatment,[33] and substrate used in thin-film formation.[32] Potassium-deficient and/or tantalum-rich KTN samples are most likely to initially crystallize as a pyrochlore, whereas niobium-rich materials form perovskite directly.[15,17,32,34] In the case of the inhomogeneous sol−gel route, the formation of a pyrochlore that is difficult to transform to perovskite is consistent with the presence of a tantalum-rich component in the gel.

The diffraction patterns for the samples prepared using the mixed oxide method indicate that sample C3 is probably a physical mixture of tantalum- and niobium-rich phases. High levels of compositional inhomogeneity in KTN specimens lead to phase coexistence as the temperatures at which the various phase transitions occur in this solid solution system are strongly dependent on the composition. Thus, at room temperature, a specimen that is essentially a mixture of KT and KN grains will give a powder diffraction pattern with contributions from cubic tantalum-rich and orthorhombic niobium-rich components.

**EXAFS Studies.** *Compositional Homogeneity of the Dry Gels.* Nb K-edge FT magnitudes for the KTN 50:50 dry gels prepared by both the homogeneus and the inhomogeneous routes are compared with those for a KN dry gel in Figure 1a. The peaks below 1 Å are of no structural significance and probably arise from multielectron excitations.[35,36] Backscattering from the first oxygen shell gives rise to peaks in the 1−2 Å region. In the metal backscattering region, the FT magnitude for the $KNbO_3$ dry gel is different from those of the KTN dry gels, suggesting that both KTN gels contain some Nb−O−Ta links. Additionally, the FT magnitudes of the KTN dry gels are different from each other, suggesting that they contain differing numbers of Nb−O−Ta links.

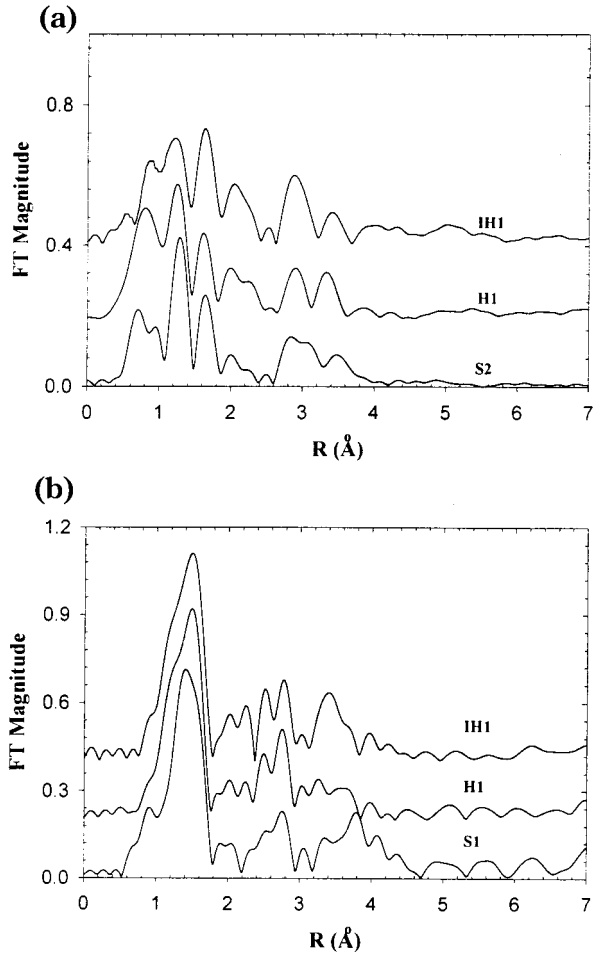


**Figure 1.** (a) Nb K-edge and (b) Ta $L_{III}$-edge Fourier transform magnitudes for KTN 50:50 dry gels prepared by the homogeneous (H1) and inhomogeneous (IH1) methods compared to those for KN (S2) and KT (S1) dry gels. The Nb and Ta Fourier transforms were performed over the ranges 1−15 and 1−17 $Å^{-1}$, respectively.

The Ta $L_{III}$-edge data for these samples also support these conclusions. The FT magnitudes for a $KTaO_3$ and two $K(Ta_{0.5}Nb_{0.5})O_3$ dry gels are shown in Figure 1b. The oxygen backscattering signals at ∼1.5 Å are similar for all of the samples, but pronounced differences in the metal backscattering region suggest that there are Ta−O−Nb links in both of the KTN dry gels and that the materials prepared by the homogeneous and inhomogeneous routes are different from one another. Although it is widely stated that sol−gel chemistry can produce materials that are compositionally homogeneous on a short length scale, it is difficult to demonstrate directly

(30) Dimakis, N.; Bunker, G. *Phys. Rev. B* **1998**, *58*, 2467−2475.
(31) Nazeri, A. *Appl. Phys. Lett.* **1994**, *65*, 295−297.
(32) Nazeri, A.; Kahn, M. *J. Am. Ceram. Soc.* **1992**, *75*, 2125−2133.
(33) Nazeri, A.; Kahn, M.; Bender, B.; Allen, C. *J. Am. Ceram. Soc.* **1994**, *77*, 2450−2454.
(34) Nazeri-Eshghi, A.; Kuang, A. X.; Mackenzie, J. D. *J. Mater. Sci.* **1990**, *25*, 3333−3337.
(35) Bridges, F.; Booth, C. H.; Li, G. G. *Phys. B* **1995**, *208 & 209*, 121−124.
(36) Wang, W.-C.; Chen, Y. *Phys. Status Solidi A* **1998**, *168*, 351−357.

that heterocondensation (M−O−M′ link formation, where M and M′ are different metals) has occurred during sol or gel formation. Both EXAFS[8,37−39] and NMR experiments have been used to examine this issue. Although there are examples for which an NMR examination of a "metal" nucleus, such as $^{29}Si$, has been useful, $^{17}O$ NMR spectroscopy seems to be a particularly powerful approach.[40] $^{17}O$ chemical shifts are very sensitive to the immediate coordination environment,[41] and this sensitivity has been used to study the compositional homogeneity of sol−gel-processed materials such as $TiO_2$−$SiO_2$,[42,43] $ZrO_2$−$SiO_2$,[44] $Ta_2O_5$−$SiO_2$,[45] and inorganic−organic hybrid silicates.[40,46]

*Evolution of the Local Structure on Crystallization*. Only the crystalline samples (H3, H4, IH3, and IH4) showed strong features in their Nb K-edge and Ta $L_{III}$-edge FT magnitudes due to backscattering from both potassium (∼3 Å) and transition metal neighbors (3−4 Å). The spectra for the crystalline samples (H3 and H4) are very different from those of the amorphous materials and are almost identical to each other, indicating that the local structure around the absorber does not change significantly on heating once the perovskite has crystallized. This is also true for the samples made using prehydrolyzed precursors.

*Quantitative Analysis of the Nb−O EXAFS Data*. A 3 + 3 coordination model, similar to that for niobium in $KNbO_3$, was initially used in fitting the data for all of the samples. Good fits were achieved for the crystalline KTN samples, but a poor fit to the data for the amorphous materials suggested that a different model was needed. There have been reports of distorted octahedral coordination for Nb in crystals isolated from niobium-containing alkoxide solutions.[47−49] A 3 + 1 + 2 coordination model based on these studies was explored for the amorphous samples. $\Delta E_0$ for these analyses was obtained by fitting the $KNbO_3$ data. The parameters obtained from the analyses are given in Table 2, and the fits to the Fourier-filtered Nb−O EXAFS are shown in Figure 2a. The model was not entirely satisfactory as some of the Debye−Waller factors were unreasonably large. However, an inspection of the results indicates that the coordination environment of the niobium (i) changes prior to crystallization (H1 and H2 are quite different, see Figure 2a); (ii) differs for the niobium in the samples prepared by the inhomogeneous and homogeneous methods; and (iii) in the KN (sample S2) and KTN 50:50 (sample H1), dry gels consists of oxygen neighbors with at least two markedly different Nb−O distances. The Nb−O EXAFS for the latter samples show a beat at around 8 $Å^{-1}$. The average Nb−O distances apparently change little on crystallization, suggesting that the coordination number of the niobium does not change.

**Table 2. Nb K-Edge EXAFS Analysis Results for the Oxygen Shell**

| sample ID | $N^a$ | $R$ (Å) | $\sigma^2$ ($Å^2$) | $R_{ave}$ (Å) |
|---|---|---|---|---|
| S2 | 3 | 1.884(3) | 0.0043(4) | 1.992 |
| | 1 | 2.029(4) | 0.0024(4) | |
| | 2 | 2.136(5) | 0.0021(7) | |
| H1 | 3 | 1.896(4) | 0.0105(5) | 2.013 |
| | 1 | 2.051(4) | 0.0016(4) | |
| | 2 | 2.169(9) | 0.0108(14) | |
| H2 | 3 | 1.886(4) | 0.0047(5) | 2.003 |
| | 1 | 2.044(3) | 0.0042(3) | |
| | 2 | 2.157(4) | 0.0010(4) | |
| H3 | 3 | 1.905(3) | 0.0051(3) | 2.001 |
| | 3 | 2.098(3) | 0.0040(3) | |
| H4 | 3 | 1.914(3) | 0.0044(3) | 2.011 |
| | 3 | 2.108(3) | 0.0036(3) | |
| H6 | 3 | 1.915(2) | 0.0011(2) | 2.005 |
| | 3 | 2.095(3) | 0.0007(2) | |
| H7 | 3 | 1.909(3) | 0.0038(3) | 2.013 |
| | 3 | 2.116(4) | 0.0044(4) | |
| IH1 | 3 | 1.906(6) | 0.0130(7) | 2.014 |
| | 1 | 2.048(3) | 0.0054(2) | |
| | 2 | 2.160(13) | 0.0139(16) | |
| IH2 | 3 | 1.888(7) | 0.0109(17) | 1.999 |
| | 1 | 2.038(3) | 0.0032(4) | |
| | 2 | 2.147(8) | 0.0075(12) | |
| IH3 | 3 | 1.884(3) | 0.0041(2) | 1.984 |
| | 3 | 2.085(4) | 0.0056(4) | |
| IH4 | 3 | 1.884(2) | 0.0031(2) | 1.984 |
| | 3 | 2.085(3) | 0.0042(3) | |
| C3 | 3 | 1.894(2) | 0.0039(3) | 1.980 |
| | 3 | 2.132(3) | 0.0039(3) | |
| C4 | 3 | 1.915(2) | 0.0029(2) | 2.021 |
| | 3 | 2.127(2) | 0.0024(2) | |

[a] $N$ is the number of backscattering oxygen atoms at a distance $R$ from the absorber.

*Quantitative Analysis of the Ta−O EXAFS Data for the Amorphous Samples*. Initially, a single-shell model was explored. The fits were poor and gave unreasonably large values for $\sigma^2$ (Debye−Waller factor), indicating that a model with subshells was needed. Several two- and three-subshell models were then examined. $\Delta E_0$ for these analyses was obtained by fitting the data for crystalline $KTaO_3$. A model with 3 + 2 + 1 coordination was adopted for the final analyses, although in some cases the thermal parameters were rather high. This latter type of coordination environment for Ta has previously been observed in the complex $Mo_3Ta_2O_8(O^i\text{-}Pr)_{10}$, which was isolated from metal isopropoxide mixtures.[47] The fits to the Fourier-filtered EXAFS data are shown in Figure 2b, and the resulting parameters are summarized in Table 3. The Ta−O EXAFS results change when the samples are heated prior to crystallization, suggesting a change in coordination geometry as the residual organics are burned out of the gel. In contrast to the Nb−O EXAFS data, there is no evidence of a beat in any of the Ta−O EXAFS results, indicating that the dominant groups of backscattering oxygen

(37) Ahlfanger, R.; Bertagnolli, H.; Ertel, T.; Kolb, U.; Peter, D.; Nass, R.; Schmidt, H. *Der. Bunsen-Ges. Phys. Chem.* **1991**, *95*, 1286−1289.
(38) Arcon, I.; Malic, B.; Kodre, A.; Kosec, M. *J. Synchrotron Radiat.* **1999**, *6*, 535−536.
(39) Xu, J.; Pattanaik, S.; Lind, C.; Wilkinson, A. P. *Chem. Mater.* **2000**, *12*, 3347−3355.
(40) Babonneau, F.; Maquet, J. *Polyhedron* **2000**, *19*, 315−322.
(41) Bastow, T. J.; Dirken, P. J.; Smith, M. E.; Whitfield, H. J. *J. Phys. Chem.* **1996**, *100*, 18539−18545.
(42) Dirken, P. J.; Smith, M. E.; Whitfield, H. J. *J. Phys. Chem.* **1995**, *99*, 395−401.
(43) Holland, M. A.; Pickup, D. M.; Mountjoy, G.; Tsang, E. S. C.; Wallidge, G. W.; Newport, R. J.; Smith, M. E. *J. Mater. Chem.* **2000**, *10*, 2495−2501.
(44) Pickup, D. M.; Mountjoy, G.; Wallidge, G. W.; Newport, R. J.; Smith, M. E. *Phys. Chem. Chem. Phys.* **1999**, *1*, 2527−2533.
(45) Pickup, D. M.; Mountjoy, G.; Holland, M. A.; Wallidge, G. W.; Newport, R. J.; Smith, M. E. *J. Mater. Chem.* **2000**, *10*, 1887−1894.
(46) Lebeau, B.; Maquet, J.; Sanchez, C.; Beaume, F.; Laupretre, F. *J. Mater. Chem.* **1997**, *7*, 989−995.
(47) Johansson, A.; Roman, M.; Seisenbaeva, G. A.; Kloo, L.; Szabo, Z.; Kessler, V. G. *J. Chem. Soc., Dalton Trans.* **2000**, 387−394.
(48) Kessler, V. G.; Turova, N. Y.; Yanovskii, A. I.; Belokon, A. I.; Struchkov, Y. T. *Russ. J. Inorg. Chem.* **1991**, *36*, 938−944.
(49) Boyle, T. J.; Alam, T. M.; Dimos, D.; Moore, G. J.; Buchheit, C. D.; Al-Shareef, H. N.; Mechenbier, E. R.; Bear, B. R.; Ziller, J. W. *Chem. Mater.* **1997**, *9*, 3187−3198.

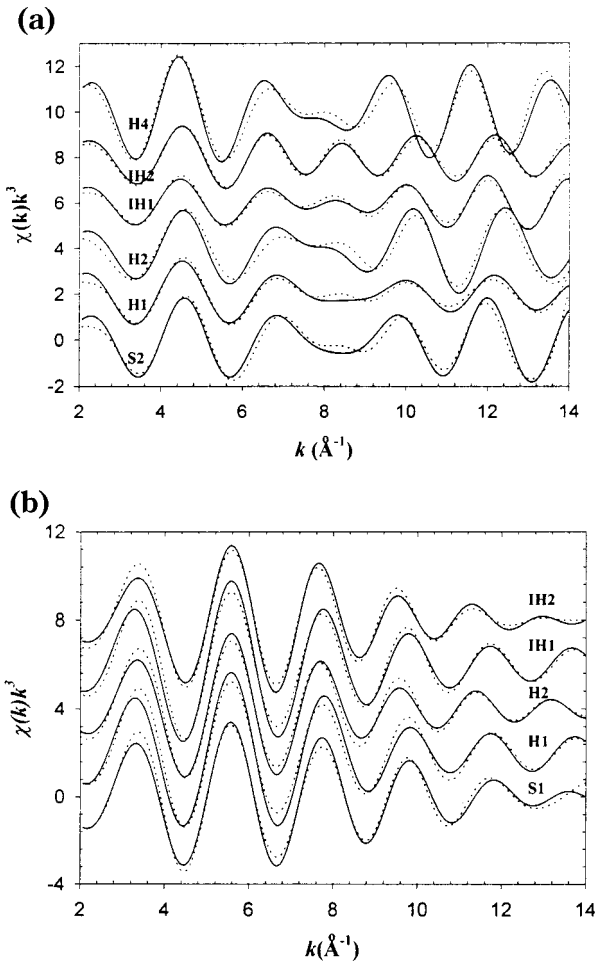


**Figure 2.** Fits to (a) the Nb−O EXAFS for a KN dry gel (S2) and several amorphous KTN 50:50 samples and (b) the Ta−O EXAFS for a KT dry gel (S1) and the same series of KTN 50:50 samples. Observed and calculated values are indicated by the solid and dotted lines, respectively.

**Table 3. Ta $L_{III}$-Edge EXAFS Analysis Results for the Oxygen Shell**

| sample ID | $N^a$ | R (Å) | $\sigma^2$ (Å$^2$) |
|---|---|---|---|
| S1 | 3 | 1.924(2) | 0.0026(3) |
| | 2 | 2.055(3) | 0.0018(4) |
| | 1 | 2.223(8) | 0.0039(9) |
| H1 | 3 | 1.926(2) | 0.0037(2) |
| | 2 | 2.048(4) | 0.0045(6) |
| | 1 | 2.211(14) | 0.0089(21) |
| H2 | 3 | 1.937(5) | 0.0090(9) |
| | 2 | 2.014(8) | 0.0051(4) |
| | 1 | 2.263(19) | 0.0102(10) |
| H3 | 6 | 2.000(6) | 0.0114(9) |
| H4 | 6 | 1.991(6) | 0.0097(10) |
| H6 | 6 | 1.990(4) | 0.0065(5) |
| H7 | 6 | 1.984(7) | 0.0124(20) |
| H8 | 6 | 1.993(5) | 0.0036(5) |
| IH1 | 3 | 1.930(2) | 0.0039(2) |
| | 2 | 2.048(4) | 0.0051(7) |
| | 1 | 2.219(16) | 0.0105(25) |
| IH2 | 3 | 1.938(2) | 0.0060(5) |
| | 2 | 2.050(4) | 0.0042(5) |
| | 1 | 2.336(9) | 0.0077(13) |
| IH3 | 6 | 1.985(5) | 0.0081(7) |
| IH4 | 6 | 1.992(5) | 0.0084(7) |
| C3 | 6 | 1.994(4) | 0.0055(6) |
| C4 | 6 | 1.987(4) | 0.0046(4) |

[a] *N* is the number of backscattering oxygen atoms at a distance *R* from the absorbing atom.

atoms are at similar M−O distances. The coordination polyhedron for the tantalum is apparently less dramatically distorted than that of the niobium. The average Ta−O bond lengths for all of the amorphous samples are similar to one another (∼2.02 Å) and only slightly longer than those observed for $Mo_3Ta_2O_8(O^iPr)_{10}$ (∼1.98 Å) and crystalline $KTaO_3$ (∼1.99 Å). This suggests that there is no change in coordination number on crystallization.

*Sensitivity of EXAFS to Changes in Local Composition*. The Nb K-edge FT magnitudes for a series of crystalline KTN samples with different compositions are shown in Figure 3a. The appearance of the metal backscattering region (3−4 Å) changes dramatically as the Nb content of the samples increases from 33 to 100%, indicating that this peak is very sensitive to the average number of tantalum and niobium nearest neighbors around the absorbing atom. The Ta $L_{III}$-edge FT magnitudes for the crystalline KTN samples also show a strong dependence on solid-solution composition (see Figure 3b). The peak in the transition metal backscattering region becomes weaker and splits as more niobium is introduced into the solid solution. At niobium concentrations >67%, the peak becomes stronger again. This is because of the destructive interference between tantalum and niobium backscattering at intermediate concentrations. This is illustrated in Figure 3c, where $k^3\chi(k)$ for the metal backscattering region (3−4 Å) is shown for each of the compositions studied. The tantalum EXAFS signals for the $KTaO_3$ and $KTa_{0.04}Nb_{0.96}O_3$ samples are out of phase with one another, so that intermediate compositions have a reduced overall amplitude. The figure also shows that the position of the maximum in the amplitude envelope varies with composition. $k_{max}$ shifts from ∼14 Å$^{-1}$ for the 4% Ta sample to ∼16 Å$^{-1}$ for the 100% Ta material.

*Qualitative Evaluation of Sample Homogeneity*. As both the Nb K-edge and Ta $L_{III}$-edge FT magnitudes are very sensitive to the nature of the nearest-neighbor transition metals, a qualitative examination of the influence of processing chemistry on sample heterogeneity was undertaken by comparing the FT magnitudes for samples prepared in different ways.

The influence of processing chemistry on the Nb K-edge FT magnitudes for a series of KTN 50:50 samples that had been prepared in different ways is shown in Figure 4a and b. In the transition metal backscattering region (3−4 Å), the FT magnitude for the 50:50 sample prepared by the inhomogeneous method (IH4) differs markedly from that for the 50:50 sample prepared by the homogeneous route (H4), but it is similar to that for the 33:67 sample prepared by the homogeneous method (H7). This implies that the cation distributions in samples H4 and IH4 are different and that, assuming that the samples prepared by the homogeneous sol−gel route are random solid solutions, the niobium in sample IH4 has, on average, close to two tantalum and four niobium atoms in its first shell of transition metal neighbors.

The Ta $L_{III}$-edge data provide support for these conclusions. The Ta $L_{III}$ FT magnitudes for the series of KTN samples are shown in Figure 5a−c. In the transition metal backscattering region (3−4 Å), the Ta $L_{III}$-edge FT magnitude for the 50:50 sample prepared by the inhomogeneous method (IH4) differs markedly from that for the 50:50 sample prepared by the homogeneous route (H4), but it is similar to that for the 67:

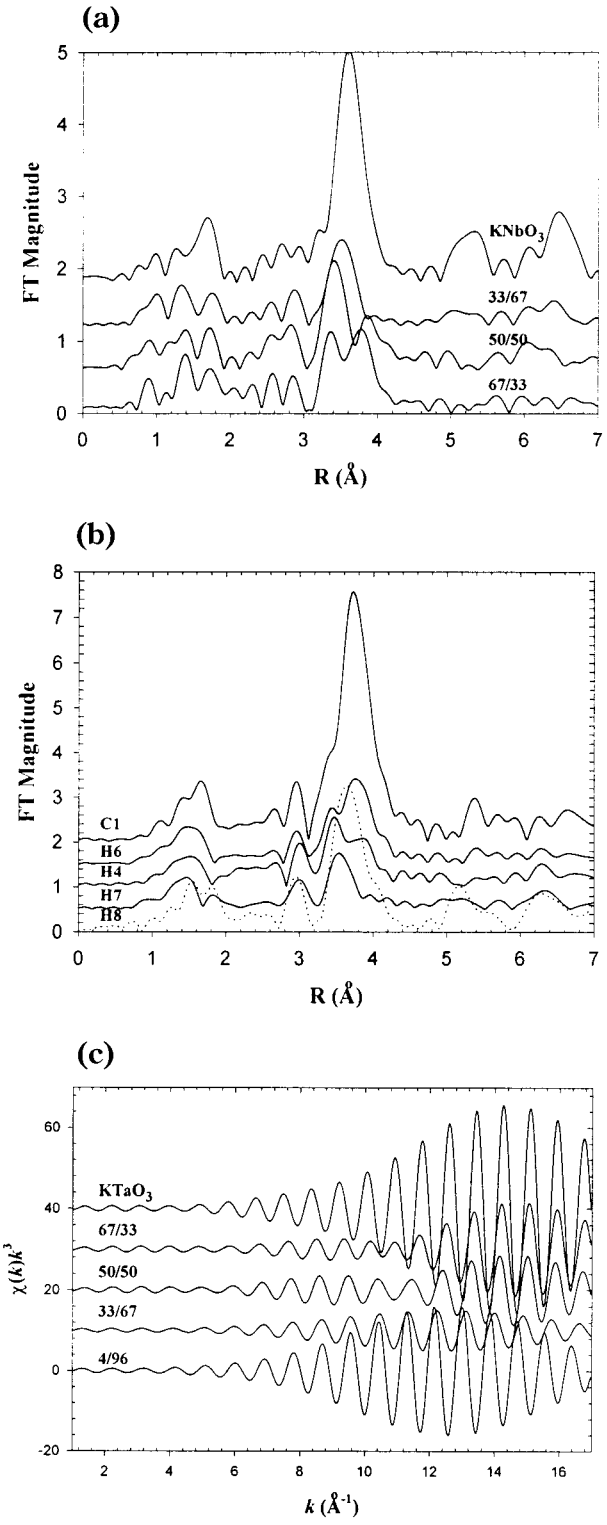


**Figure 3.** (a) Nb K-edge and (b) Ta $L_{III}$-edge Fourier transform magnitudes for different KTN compositions. (c) The corresponding Ta $L_{III}$-edge EXAFS. All of the Fourier transforms were performed over the range 1−17 $Å^{-1}$.

33 sample prepared by the homogeneous method (H6). This implies that the cation distributions in samples H4 and IH4 are different and that, assuming that the samples prepared by the homogeneous sol−gel route are random solid solutions, the tantalum in sample IH4 has, on average, close to four tantalum and two niobium atoms in its first shell of transition metal neighbors.

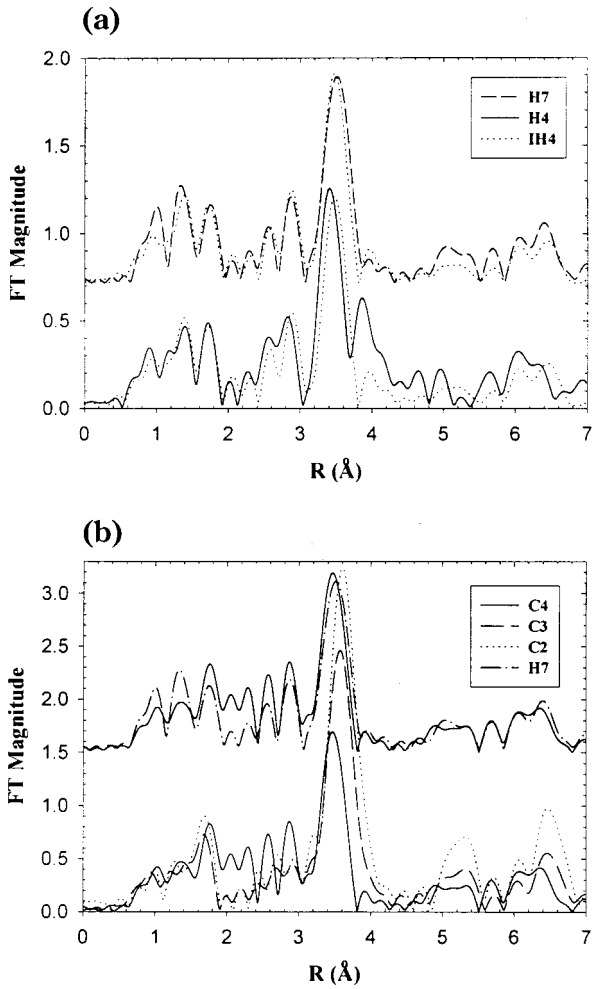


**Figure 4.** Nb K-edge Fourier transform magnitudes for perovskite KTN samples prepared using (a) different sol−gel routes and (b) different mixed oxide methods. The Fourier transforms were performed over the range 1−17 $Å^{-1}$.

The samples prepared by the mixed oxide method also displayed very different FT magnitudes. The Nb K-edge FT magnitudes for these samples are shown in Figure 4b, and the corresponding Ta $L_{III}$-edge FT magnitudes are shown in Figure 5b. In the transition metal backscattering region, the Nb FT magnitude for sample C4 (KTN 50:50 repeatedly ground and heated) closely resembled that for sample H7 (homogeneous sol−gel 33:67), and the FT magnitude for sample C3 (KTN 50:50 loose fired without intermediate regrinding) appeared to be intermediate between those for pure $KNbO_3$ and sample C4. The Ta $L_{III}$ FT magnitude for sample C4 closely resembled that for sample H6 (homogeneous sol−gel 67:33, see Figure 5c), and the FT magnitude for sample C3 appeared to be intermediate between those for pure $KTaO_3$ and sample C4. These observations suggest that sample C3 is more inhomogeneous than sample C4 and that even C4 is not perfectly homogeneous. The presence of large amounts of inhomogeneity in sample C3 was also supported by our X-ray diffraction measurements.

*Influence of Heating Time on Compositional Heterogeneity*. The effect of heating time on the cation distribution in the crystalline KTN 50:50 samples prepared by the inhomogeneous sol−gel route was examined. These materials had been heated at 1000 °C for 1, 2, 4,

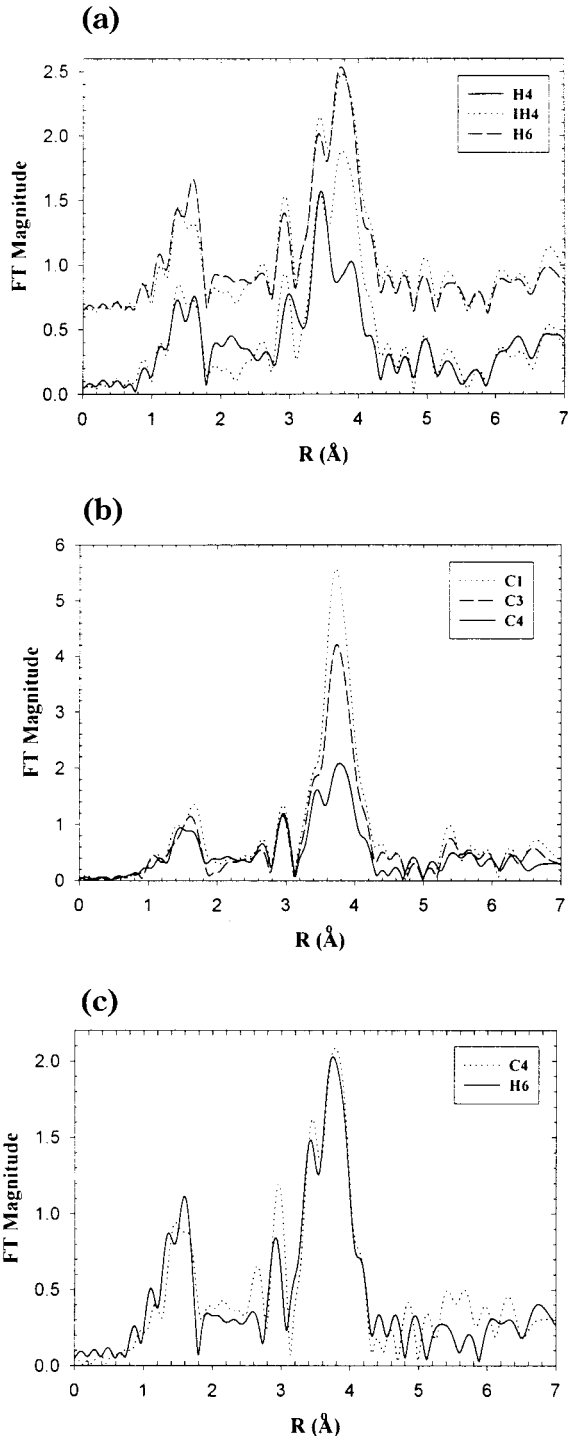


**Figure 5.** Ta $L_{III}$-edge Fourier transform magnitudes for perovskite KTN samples prepared using (a) different sol−gel routes and (b) different mixed oxide methods. (c) A comparison of the FT magnitude for a KTN 50:50 mixed oxide sample (C4) with that for a KTN 67:33 conventional sol−gel sample (H6). The FTs were performed over the range 1−17 $Å^{-1}$.

and 8 h. The metal backscattering regions in the FTs were all similar, indicating that the average number of Nb and Ta atoms around the absorber does not change on heating. This suggests that the compositional heterogeneity that is present in these samples is on a sufficiently long length scale that it cannot be eliminated by heating at 1000 °C for short periods of time.

*Quantitative Evaluation of Sample Homogeneity.* Although our comparison of the FT magnitudes for different KTN samples provides interesting qualitative information, it is desirable to quantify the heterogeneity of the materials. An analysis of the Ta $L_{III}$-edge EXAFS data including the transition metal backscattering was attempted by including multiple scattering paths in the model. For all of the crystalline KTN samples, one oxygen scattering path, one potassium scattering path, two transition metal single scattering paths (Ta−Ta and Ta−Nb), and four multiple scattering paths (Ta−$O_1$−$Ta_3$, Ta−$O_1$−$Nb_3$, Ta−$O_1$−$Ta_3$−$O_1$, and Ta−$O_1$−$Nb_3$−$O_1$) were employed. Good fits were achieved by varying the path lengths, Debye−Waller factors, and coordination numbers while using the constraints described in the Experimental Section (see Figure 6 for example fits). The key parameters resulting from the analyses are summarized in Tables 3 and 4. Ta−O distances of ∼1.99 Å were obtained in every case, in good agreement with the value for $KTaO_3$ (1.994 Å). The analyses indicate that, on average, the absorbing tantalum atoms in the $K(Ta_{0.04}Nb_{0.96})O_3$, $K(Ta_{0.33}Nb_{0.67})O_3$, $K(Ta_{0.5}Nb_{0.5})O_3$, and $K(Ta_{0.67}Nb_{0.33})O_3$ samples prepared by the homogeneous sol−gel route have 0.5/5.5, 2.0/4.0, 3.2/2.8, and 3.8/2.2 (Ta/Nb) nearest neighbors, respectively. These values are very close to those expected for a random solid solution, namely, 0.24/5.76, 2/4, 3/3, and 4/2, respectively (see Table 4). For the $K(Ta_{0.5}Nb_{0.5})O_3$ sample prepared by the inhomogeneous sol−gel route, the average numbers of Ta/Nb nearest neighbors around tantalum were estimated to be 3.9/2.1, which is in good agreement with the conclusions from our qualitative analyses. The analyses for the samples prepared by two different mixed oxide methods indicated that, for samples C3 and C4, the average numbers of Ta/Nb nearest neighbors around tantalum were 5.3/0.7 and 3.8/2.2, respectively. These results are again in good agreement with the qualitative analyses.

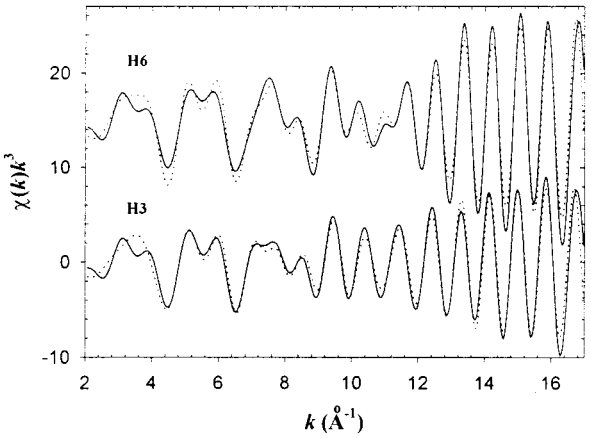


**Figure 6.** Examples of the multiple scattering fits to the Ta $L_{III}$-edge data for KTN perovskites. The observed and calculated $\chi(k)k^3$ values are represented by solid and dashed lines, respectively.

*Validation of the Metal Backscattering Quantitative Analyses.* The analyses of the transition metal backscattering in the Ta $L_{III}$-edge EXAFS data were performed using a model for the average metal environment, rather than using a model consisting of a weighted average of all of the possible metal environments, $Ta_0Nb_6$, $Ta_1Nb_5$, $Ta_2Nb_4$, $Ta_3Nb_3$, $Ta_4Nb_2$, $Ta_5Nb_1$, and $Ta_6Nb_0$ (the subscript refers to the number of cations in the shell). This should be a valid approach provided that

**Table 4. Ta $L_{III}$-Edge EXAFS Analysis Results for the Transition Metal Shell**

| sample ID | composition | atomic pair | $R$ (Å) | $N^a$ (Ta/Nb) | $\sigma^2$ (Å$^2$) |
|---|---|---|---|---|---|
| C1 | $KTaO_3$ | Ta−Ta | 3.988 | 6 | 0.0021(2) |
| C3 | $K(Ta_{0.5}Nb_{0.5})O_3$ | Ta−M | 3.986(7) | 5.3/0.7(7) | 0.0032(8) |
| C4 | $K(Ta_{0.5}Nb_{0.5})O_3$ | Ta−M | 4.014(7) | 3.8/2.2(6) | 0.0009(5) |
| H3 | $K(Ta_{0.5}Nb_{0.5})O_3$ | Ta−M | 3.986(1) | 3.2/2.8(3) | 0.0024(2) |
| H4 | $K(Ta_{0.5}Nb_{0.5})O_3$ | Ta−M | 3.981(2) | 3.2/2.8(3) | 0.0021(3) |
| H6 | $K(Ta_{0.67}Nb_{0.33})O_3$ | Ta−M | 4.018(5) | 3.8/2.2(10) | 0.0011(5) |
| H7 | $K(Ta_{0.33}Nb_{0.67})O_3$ | Ta−M | 4.021(3) | 2.0/4.0(9) | 0.0028(6) |
| H9 | $K(Ta_{0.04}Nb_{0.96})O_3$ | Ta−M | 4.019(3) | 0.5/5.5(12) | 0.0036(8) |
| IH3 | $K(Ta_{0.5}Nb_{0.5})O_3$ | Ta−M | 4.023(7) | 3.5/2.5(8) | 0.0012(4) |
| IH4 | $K(Ta_{0.5}Nb_{0.5})O_3$ | Ta−M | 4.024(4) | 4.2/1.8(4) | 0.0008(2) |
| IH5 | $K(Ta_{0.5}Nb_{0.5})O_3$ | Ta−M | 4.013(4) | 3.8/2.2(3) | 0.0008(4) |
| IH6 | $K(Ta_{0.5}Nb_{0.5})O_3$ | Ta−M | 4.014(7) | 3.7/2.3(8) | 0.0008(3) |
| IH7 | $K(Ta_{0.5}Nb_{0.5})O_3$ | Ta−M | 4.012(6) | 3.7/2.3(6) | 0.0008(2) |
| IH8 | $K(Ta_{0.5}Nb_{0.5})O_3$ | Ta−M | 4.014(5) | 3.8/2.2(4) | 0.0008(2) |

[a] $N$ is the number of transition metal Ta/Nb neighbors around the absorber.

noncollinear multiple scattering paths do not make a significant contribution to the EXAFS signals. We verified that our approach was reasonable by comparing a weighted average (weights chosen for a random 50:50 KTN solid solution) of the simulated EXAFS signals for the different possible environments ($Ta_0Nb_6$, $Ta_1Nb_5$, $Ta_2Nb_4$, $Ta_3Nb_3$, $Ta_4Nb_2$, $Ta_5Nb_1$, and $Ta_6Nb_0$) and their different isomeric forms with that calculated for the average tantalum environment for a KTN 50:50 solid solution (three tantalum and three niobium neighbors). The two approaches were in excellent agreement, indicating that the use of an average metal environment model is reasonable.

*Influence of Processing Chemistry on Solid Solution Homogeneity*. The quantitative analyses for the Ta $L_{III}$-edge EXAFS data suggest that all of the KTN samples prepared using the homogeneous sol−gel procedure are compositionally homogeneous random solid solutions. Although compositional homogeneity is typically expected for materials produced using sol−gel methods, we have previously found indications that, for $Pb(Zr_{0.5}Ti_{0.5})O_3$, the most widely used sol−gel method does not necessarily produce compositionally homogeneous materials.[11] This difference between the KTN and PZT systems is not unreasonable. $Ta^{5+}$ and $Nb^{5+}$ have almost identical ionic sizes, so the hydrolysis rates for the alkoxide precursors and the rates of M−O−M′ link formation should be approximately the same for both metals, leading to compositionally homogeneous gels. However, the kinetics of hydrolysis for $Ti(OR)_4$ and $Zr(OR)_4$ are typically very different from one another, and this could lead to inhomogeneities.

Both the qualitative and quantitative examinations of inhomogeneity in the KTN 50:50 samples prepared using prehydrolyzed precursors indicate that this approach can be used to introduce inhomogeneity into a solid solution on a length scale that cannot be readily removed by annealing. Our examination of the samples prepared by the direct reaction of oxides indicated that even the material prepared using several grinding and heating cycles was inhomogeneous.

## Conclusions

EXAFS proved to a valuable tool for the examination of compositional inhomogeneities in KTN solid-solution samples. In addition to providing qualitative information, a relatively simple model was successfully used to quantitatively examine the homogeneity of the KTN samples. The results of this analysis are entirely consistent with a random distribution of tantalum and niobium in the samples prepared by the conventional sol−gel process and clearly indicate that prehydrolyzed precursors can be used to deliberately introduce heterogeneities into the final samples. Additionally, the EXAFS studies of samples prepared by repeatedly grinding and heating a mixture of oxides highlight the difficulty of preparing high-quality homogeneous solid solutions by this approach.

**Acknowledgment.** This work was primarily supported by NSF Award DMR-9623890. The authors gratefully acknowledge the use of beamline X11A at the National Synchrotron Light Source, Brookhaven National Laboratory. X11A is supported, in part, by the U.S. Department of Energy, Division of Materials Science, under Contract DE-FG02-89ER45384.

CM0004735